2020 IMEKO TC-19 International Workshop on
Metrology for the Sea
Naples, Italy, October 5-7, 2020

Kriging interpolation of bathymetric data for 3D model of the Bay of Pozzuoli (Italy)

Emanuele Alcaras[1], Claudio Parente[1], Andrea Vallario[1]

[1] *Department of Sciences and Technologies, Centro Direzionale di Napoli, Isola C4, 80143 Naples (Italy), (emanuele.alcaras, claudio.parente, andrea.vallario)@uniparthenope.it*

***Abstract* – Bathymetric data acquired by a single beam echo-sounder, as well as those derived by a navigational chart, require interpolation procedure to pass from cloud point dataset to continuous tridimensional representation. Among different algorithms available in GIS software, Kriging interpolators are very powerful tools to process bathymetric data. This paper aims to analyze the accuracy levels that can be reached using Kriging. Bathymetric information included in two Electronic Navigational Charts (ENCs) of the Bay of Pozzuoli (nominal scale 1:30.000) is used for digital 3D model of this area. Interpolation processes are performed in GIS environment (software: ArcGIS 10.3.1, including the extension Geostatistical Analyst, by ESRI); the achieved results are analyzed by varying the choice of the mathematic function for semi-variogram. The experiments carried out in this study demonstrate how the careful choice of the semi-variogram model can help to increase the accuracy of the interpolation process.**

I. INTRODUCTION

Hydrographic survey permits to acquire in water depth estimation that is fundamental for many purposes, first of all in maritime navigation: by providing possible tracks for vessels, it allows to chart safe routes that do not cross any dangerous ground. Another important purpose of hydrography is in the field of dredging, the operation of clearing the bed of a harbor, river, or other area of water by scooping out mud, weeds, and rubbish. The knowledge of the seabed is useful in determining shorelines that extend around a coast, suitable to support studies on the effect of water bodies on land, to predict possible flooding zones and to suggest measures to effectively counter this [1].

Hydrographic survey can be carried out by using different techniques. Single beam sonar (SBS) and multi beam sonar (MBS) determine the depth of any waterbody by using sound beams. Particularly, they measure the time lag between transmitting and receiving a signal that travels through the water, springs back the seafloor, and returns to the sounder; the time lag is converted into a range using the known speed of sound [2]. SBS is a less expansive system that MBS, but provides much lower spatial resolution [3]. A good level of information about seabed morphology can be extract by multispectral satellite images, even if only in shallow water (depths less than 20 meters) [4].

The results of bathymetric survey are used for nautical charts that provide seabed morphology through depth points and contours. Available in digital form (raster or vector), nautical charts are legible and manageable by information systems supporting ship navigation, i.e. Electronic Charting Systems (ECSs) and Electronic Chart Display and Information Systems (ECDISs) [5].

Regardless of the technique with which they are obtained and the source from which they are extracted, data concerning seabed morphology can be used to produce bathymetric model that, according to International Hydrographic Organization (IHO), can be defined, as ‘‘a digital representation of the topography (bathymetry) of the seafloor by coordinates and depths’’ [6].

When a point cloud dataset is available, i.e. single beam data or depth data derived from a nautical chart, an interpolation process is necessary to generate a 3D model: starting from irregular spaced measured points, the depths in unsampled areas must be calculated, using appropriate grid spacing related to the accuracy of the input data. However, it is possible to pass from high to low resolution model using generalization algorithms available in literature [7].

Several interpolation methods are offered by GIS software to interpolate depth values, but in many cases, the most performing ones result Kriging interpolators, i.e. Ordinary Kriging, Universal Kriging and Simple Kriging [2]. They cannot be applied in automatic way, but require the supervision of the user to set specific parameters.

The aim of this article is to demonstrate that the level of accuracy that can be achieved depends crucially on the choice of one of these parameters, that is the mathematical model of the semi-variogram, a graphical representation of the spatial correlation between the measurement points.

This paper is organized as follows. Section 2 describes the experimental framework used to evaluate the relevance of the semi-variogram on the model resulting from kriging application. Section 3 introduces and discusses the results. Finally, Section 4 presents our

conclusions.

II. DATA AND METHODS

In order to pursue an empirical study, we have identified the Bay of Pozzuoli as a study area subject to 3D modeling of the seabed. Located in the northwestern end of the Gulf of Naples in the Tyrrhenian Sea, it lies west of Naples and is dominated by the port of Pozzuoli.

The study area and its location in the Gulf of Naples are reported in Fig. 1.

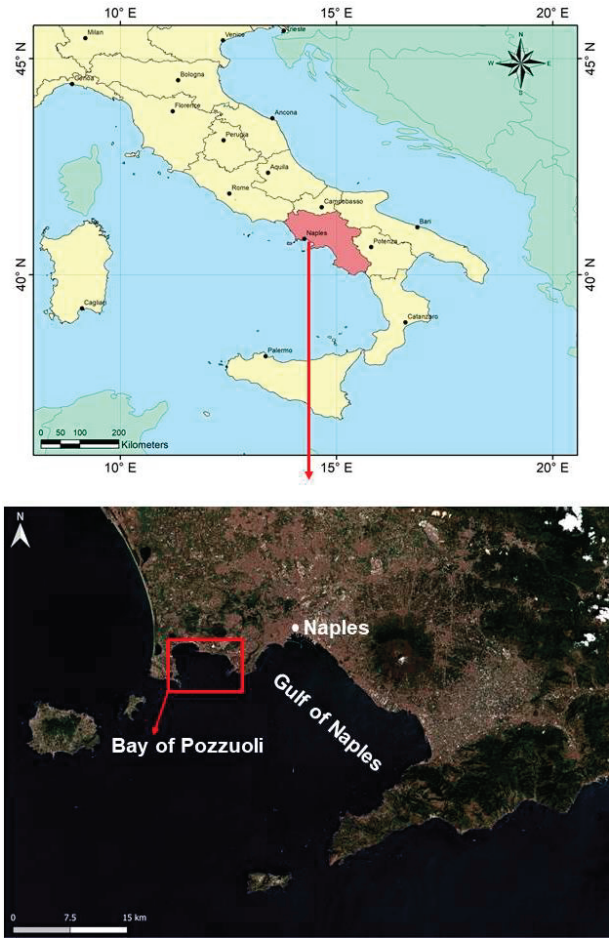

Fig. 1. Geo-localization of the Bay of Pozzuoli in the national context (upper) and in the Gulf of Naples (lower).

Pozzuoli inland zone and Pozzuoli Bay are included in the active volcanic sector named "Campi Flegrei": this shallow marine area has been active since at least 78 thousand years (ka) before present (B.P.), and is characterized by at least one large caldera collapse structure [8]. The caldera extends over an area of 8 km in diameter in the central sector and is associated with the eruption of the Neapolitan Yellow Tuff (NYT), an ignimbrite deposit dated 15 ka B.P. [9].

In the Bay of Pozzuoli, the inner continental shelf, that extends between 0 – 40 m below sea level (b.s.l.), varies significantly, from a few hundred meters at its western side (Baia) to 1.6 km at its eastern side (between Bagnoli and Nisida), reaching 1.8 km west of Pozzuoli [10]. In the seabed morphology, gentle slopes prevail, and several terraced surfaces mostly oriented N130°E occur: those terraced areas present widths up to 1.5 km in the easternmost side of the Bay and as small as 0.5 km in the west [8]. Particularly, a sequence of stepped terraced surfaces located at water depth of 10, 25 and 35 m over a distance of about 4 km, is located in the inner sector of the continental shelf [11].

Studies supported by high-resolution multi beam echo-sounder survey of the Bay of Pozzuoli, joined with interpretation of reflection seismic and gravity core data, revealed a major morphologic feature of the Pozzuoli Bay, characterized by a resurgent dome, about 5 km wide in diameter, circumscribed by a 1 – 2 km wide ring fault system [10]. This feature presents a broad convex-upward profile and display an ellipsoidal shape in plain view, with axes of about 6 km and 4 km, slightly extended in WNW-ESE direction, and can be interpreted as the shallow expression of the resurgence of the inner NYT caldera [12].

The Bay of Pozzuoli is remarkable for underwater archaeology: villas, mosaics, baths, streets, houses and harbor structures of the Roman period were submerged by the sea due to the volcanism; this exceptional environment, severely sacked over the years, has been included in a Marine Protected Area since 2001 [13]. As a consequence of the overall subsidence starting at the end of the Roman period, the main part of the ancient coastal strip, including all the buildings and maritime structures, is nowadays submerged [14]. Particularly, because of the subsidence of the NYT caldera floor and sea-level rise, the remains of two settlements, Portus Iulius to the East (actually Pozzuoli area) and Baianus Lacus to the West (Baia), are present under the sea, at water depths between a few meters and 15 m b.s.l. [15].

Depth data are extracted from two Electronic Navigational Charts (ENCs) produced by the Istituto Idrografico della Marina Militare (IIMM), in scale 1:30.000, identified as n° 129 and n° 130. The two sources are necessary as the area falls half in one and half in the other nautical chart.

The original files are formed in accordance to the official standards established by the International Hydrographic Organization (S-57 IHO) [6]. They are transformed in shape file for using them in ArcGIS 10.3.1 by ESRI. ENCs are georeferred to WGS84 geodetic datum and for this study are projected in the Universal Transverse of Mercator (UTM)/WGS84 Zone 33 N. ENC depth points and contour lines in the Bay of Pozzuoli and around areas are shown in Fig. 2.

First, we group the vertices of contour lines and the depth points in one shape file; then, we select from them only ones that fall in the area shown in Fig. 3. This area

extends within the following UTM/WGS84 plane coordinates - 33T zone: E_1 = 423,500 m, E_2 = 429,000 m, N_1 = 4,514,000 m, N_2 = 4,518,500 m. Depth values range between -10 m and -115 m. Those points are used as dataset for the application of the Ordinary Kriging interpolation method available in Geostatistical Analyst [16], an extension included in ArcGIS software [17].

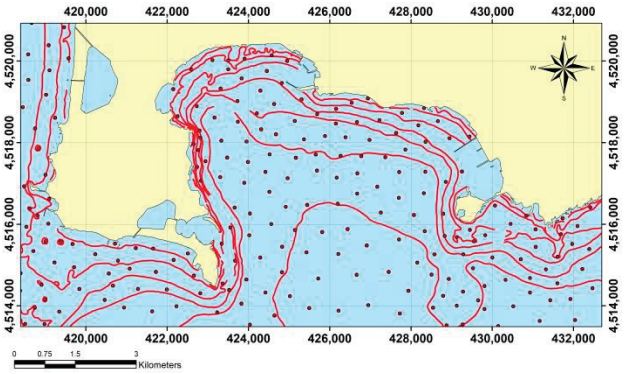

Fig. 2. ENC depth information in the Bay of Pozzuoli and around area.

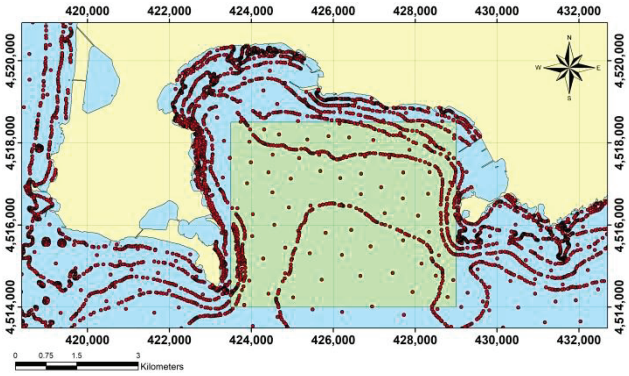

Fig. 3. The selected point dataset (in the green rectangle) submitted to Ordinary Kriging interpolation.

Kriging is founded on the first law of Geography introduced by Waldo R. Tobler's in 1969: "everything is related to everything else, but near things are more related than distant things" [18]. In other words, things closer together are more similar than things further away. Unlike to deterministic methods, Kriging applies the statistical model, which includes the spatial correlation between sampled points, and uses it to estimate the value at an unknown point: the spatial arrangement among the measured points, rather than a presumed model of spatial distribution, is used for interpolation; it also allows estimations of the uncertainty neighboring each interpolated value [19].

The spatial correlation between the measurement points can be computed using the semi-variance formula [20-21]:

$$\gamma = \frac{1}{2N(h)} \sum_{i=1}^{N(h)} [Z(u_i) - Z(u_i + h)]^2 \qquad (1)$$

Where:

- $N(h)$ is the number of pairs of measurement points with distance h apart;
- $z(u_i)$ is the value at location u_i;
- $z(u_i+h)$ is the value at location u_i+h.

The semi-variance calculated between each pair of points in the sampled data is plotted against the distance and the resulting graphical representation is called "variogram" or, since half the variance is plotted, "semi-variogram".

To facilitate the procedure and make it faster, the pairs are grouped into lag bins, e.g. the semi-variance is calculated for all pairs of points that present distance between 10 meters and 20 meters.

Mathematical models can be used to substitute the empirical ones, fitting the data in the best way, i.e. linear, gaussian, exponential, stable, etc. This substitution permits to introduce in the kriging process semi-variogram values for lag distances that are not used in the empirical semi-variogram [22].

Cross validation allows to define the accuracy level of predictive values. Particularly, leave-one-out (LOO) method is currently adopted: each point is removed in turn from the dataset and the other points are used to estimate a value at the location of the removed point; finally, the performance is tested calculating, in each removed point, the "residual" that is the difference between the known value and estimated value [23-25].

Cross validation permits also to highlight that the final shape of the spatial distribution is influenced by the choice of the semi-variance function model [26].

III. RESULTS AND DISCUSSION

In this study, ordinary Kriging is applied to the chosen dataset, by varying all mathematical semi-variogram models available in Geostatistical Analyst. Specifically, the following models are applied:

- Gaussian Model (GAM),
- Circular Model (CIM),
- Exponential Model (EXM),
- Spherical Model (SPM),
- Tetraspherical Model (TEM),
- Pentaspherical Model (PEM),
- Stable Model (STM),
- J-Bessel Model (JBM),
- K-Bessel Model (KBM),
- Rational Quadratic Model (RQM),
- Hole Effect Model (HEM).

Those models are described in literature and some of them are very recurrent in kriging applications, so the readers could referrer to specific papers on this matter,

e.g. [27-29].

Using all semi-variogram models available, eleven models are generated. In fig. 4 we report 2D representation, georeferred in UTM-WGS84 plane coordinates, for 3 of them, resulting respectively from HEM (upper), STM (middle), RQM (lower).

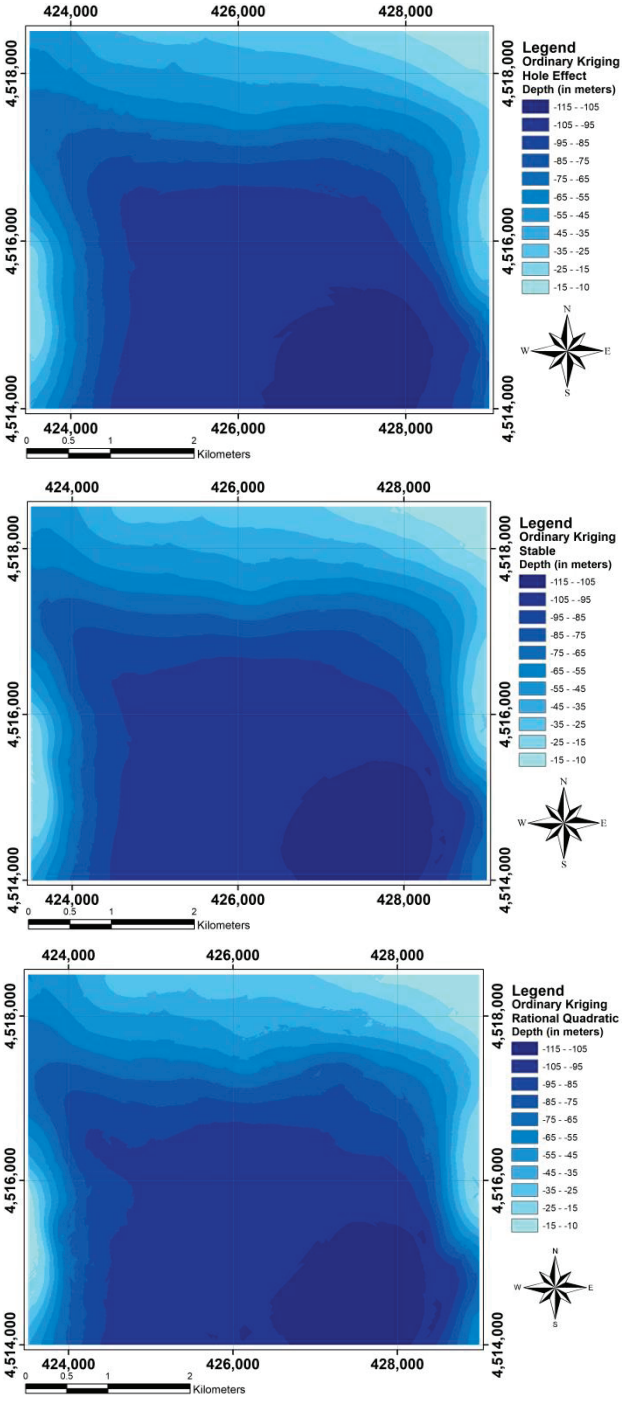

Fig. 4. 2D bathymetric models resulting from the application of: Hole Effect Semi-Variogram Model (upper), Stable Semi-Variogram Model (middle), Rational Quadratic Semi-Variogram Model (lower).

In Fig. 5, three examples of semi-variogram generated respectively by RQM (upper), CIM and GAM (lower) are shown.

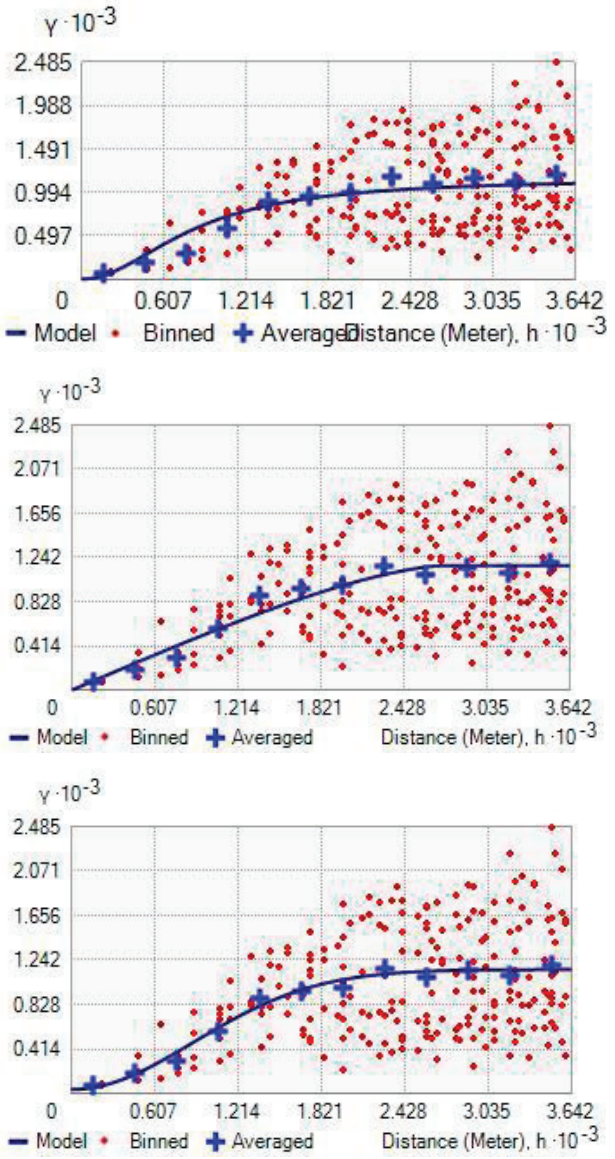

Fig. 5. Examples of semi-variograms applied to the used dataset, generated respectively by the Rational Quadratic model (upper), the Circular model (middle) and the Gaussian model (lower).

LOO cross validation is used for each kriging application on assessing the goodness of fit of the model to the empirical data. Significant statistical parameters (minimum, maximum, mean and root mean square error) of all residuals for each semi-variogram mathematical function are calculated. Those parameters are shown in table 1.

3D visualization of the most performing bathymetric model, generated by ordinary kriging interpolator with RQM, is shown in Fig. 6.

Table 1. Statistical terms of the residuals supplied by Cross validation for the ordinary kriging.

Model	Min (m)	Max (m)	Mean (m)	RMSE (m)
GAM	-14.72	11.98	-0.03	2.62
CIM	-18.79	14.43	0.09	2.01
EXM	-19.76	15.22	0.12	2.13
SPM	-18.82	14.50	0.09	2.01
TEM.	-18.83	14.47	0.09	2.01
PEM	-18.86	14.48	0.09	2.01
STM	-15.81	13.23	0.01	2.07
JBM	-15.24	11.75	-0.04	2.72
KBM	-14.99	13.58	0.00	2.18
RQM	-14.83	14.36	-0.02	1.84
HEM	-17.89	12.53	-0.06	3.24

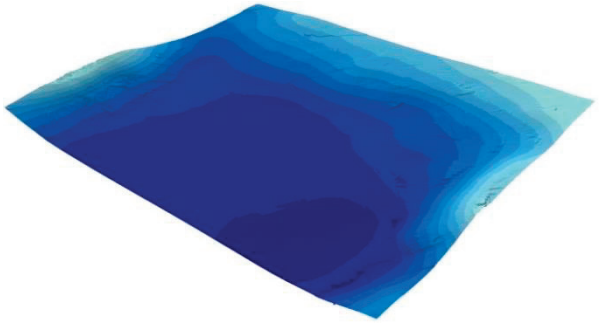

Fig. 6. 3D visualization of the most performing bathymetric model generated by ordinary kriging interpolator).

The results of the elaborations attest the different levels of accuracy than can be achieved in dependence of the choice of the semi-variogram model. Particularly, the range of minimum values goes from -14.72 m obtained for GAM, to -19.76 m resulting from EXM. The range of maximum values goes from 11.75 m obtained for JBM, to 15.22 m resulting from EXM. The range of mean values goes from -0.06 m obtained for HEM, to 0.12 m resulting from EXM. The range of RMSE goes from 1.84 m for RQM to 3.24 m resulting from HEM. By analyzing the RMSE values, RQM seems to be the most performing semi-variogram model, while HEM supplies the worst results.

The best performance of RQM obtained in this case study cannot be generalized. In other words, the comparison offers the possibility to establish in this specific case that RQM offers the best performance, but it cannot be asserted that it will always be so.

IV. CONCLUSIONS

The particular relevance of the study area, the Bay of Pozzuoli, in many fields, e.g. geology, archeology and natural science, makes clear that accurate bathymetric models are fundamental to support studies and application. To achieve this result, particular attention must be reserved to the interpolation approach to derive continuous model from cloud point dataset.

Our research remarks the high performance of the Kriging interpolation for this purpose and demonstrates the relevance of the choice of the mathematical model for the semi-variogram. As tested by using LOO cross validation, different levels of accuracy can be achieved in dependence of the function used to substitute the empirical semi-variogram, fitting the depth data in the best way. By analyzing residuals between measured and interpolated values of bathymetric depths, it is possible to identify the best performing 3D model of seabed in the study area.

The approach adopted for depth points of the Bay of Pozzuoli can be used each time bathymetric data are available and usable for 3D model of seabed. In this way, the choice of the most suitable semi-variogram model supports the user to achieve a more performing 3D bathymetric model.

REFERENCES

[1] A.Menon, "A Guide to Hydrographic Surveys", Marine Technology, Marine Insight, 2020.

[2] C.Parente, A.Vallario, "Interpolation of Single Beam Echo Sounder Data for 3D Bathymetric Model", International Journal of Advanced Computer Science and Applications, 2019, vol. 10, No 10, pp. 6-13. https://doi.org/ 10.14569/IJACSA.2019.0101002

[3] I.Parnum, J.Siwabessy, A.Gavrilov,M.Parsons, "A comparison of single beam and multibeam sonar systems in seafloor habitat mapping," Proc. 3rd Int. Conf. and Exhibition of Underwater Acoustic Measurements: Technologies & Results, Nafplion, Greece, 2009, June, pp. 155-162.

[4] C.Parente, M.Pepe, "Bathymetry from worldView-3 satellite data using radiometric band ratio," Acta Polytechnica, 2018, vol. 58, No 2, pp. 109-117. https://doi.org/10.14311/AP.2018.58.0109

[5] D.Brčić, S.Kos, S.Žuškin, Navigation with ECDIS: Choosing the proper secondary positioning source. TransNav: International Journal on Marine Navigation and Safety of Sea Transportation, 2015, 9.

[6] IHO, IHO transfer standard for digital hydrographic data - Edition 3.1 - November 2000, Special Publication No. 57, 2000, International Hydrographic Bureau, ONACO.

[7] E.Alcaras, U.Falchi, C. Parente, "Digital Terrain Model Generalization for Multiscale Use", International Review of Civil Engineering (IRECE), 2020, vol.11, No.2, pp.52-59. https://doi.org/10.15866/irece.v11i2.17815

[8] R.Somma, S.Iuliano, F.Matano, F.Molisso, S.Passaro, M.Sacchi, C.Troise, G.De Natale, "High-

resolution morpho-bathymetry of Pozzuoli Bay, southern Italy", Journal of Maps, 2016, vol.12, No. 2, pp.222-230. https://doi.org/10.1080/17445647.2014.1001800

[9] S.Carlino, R.Somma, "Eruptive versus non-eruptive behaviour of large calderas: The example of Campi Flegrei caldera (southern Italy)", Bulletin of Volcanology, 2010, vol.72, No.7, pp.871–886. https://doi.org/10.1007/s00445-010-0370-y

[10] M.Sacchi, F.Pepe M.Corradino, D.D.Insinga, F.Molisso, C.Lubritto, "The Neapolitan Yellow Tuff caldera offshore the Campi Flegrei: Stratal architecture and kinematic reconstruction during the last 15 ky", Marine Geology, 2014, vol.354, pp.15-33. https://doi.org/10.1016/j.margeo.2014.04.012

[11] M.Sacchi, F.Matano, F.Molisso, S.Passaro, M.Caccavale, G.Di Martino, A.Guarino, S.Innagi, S.Tamburrino, R.Tonielli, M.Vallefuoco, "Geological framework of the Bagnoli-Coroglio coastal zone and continental shelf, Pozzuoli (Napoli) Bay", Chemistry and Ecology, 2020, vol.36, No.6, pp.529-549.

[12] M.Sacchi, S.Passaro, R.Somma, F.Molisso, C.Violante, S.Carlino, C.Troise, G.De Natale, "The Submerged Side of the Campi Flegrei Caldera, Naples Bay, Eastern Tyrrhenian Margin", AGUFM, 2013, vol.OS33A. pp.1749.

[13] M.Stefanile, "Underwater Cultural Heritage, Tourism and Diving Centers. The case of Pozzuoli and Baiae (Italy)", In IKUWA V. Congreso Internacional de Arqueología Subacuática. Un patrimonio para la humanidad, Cartagena, 15-18 de octubre de 2014, 2016, pp.213-224.

[14] P.P.Aucelli, G.Mattei, C.Caporizzo, A.Cinque, S.Troisi, F.Peluso, M.Stefanile, G.Pappone, "Ancient coastal changes due to ground movements and human interventions in the Roman Portus Julius (Pozzuoli Gulf, Italy): Results from photogrammetric and direct surveys", Water, 2020, vol.12, No.3, pp.658.

[15] C.Morhange, N.Marriner, J.Laborel, M.Todesco, C.Oberlin, "Rapid sea-level movements and non-eruptive crustal deformation in the phlegrean Fields caldera, Italy", Geology, 2006, vol.34, pp.93–96.

[16] ESRI, Geostatistical Analyst, ArcGIS 10.3- Help, Redlands, CA, USA https://desktop.arcgis.com/en/arcmap/latest/extensions/geostatistical-analyst/what-is-arcgis-geostatistical-analyst-.htm

[17] Esri, ArcGIS 10.3, Redlands, CA, USA www.esri.com/software/arcgis

[18] W.R.Tobler, "A computer movie simulating urban growth in the Detroit region," Economic geography, 1970, vol. 46, sup1, pp. 234-240.

[19] Columbia University Mailman School of Public Health, Kriging, Columbia University, 722 West 168th St. NY, NY 10032, https://www.mailman.columbia.edu/research/population-health-methods/kriging

[20] R.A.Olea, "Geostatistics for engineers and earth scientists". Boston, Springer, ISBN 978-0-7923-8523-3, 1999, pp. 303.

[21] M.Bachmaier, M.Backes, "Variogram or semivariogram? Understanding the variances in a variogram", Precision Agriculture, 2008, Springer-Verlag, Berlin, Heidelberg, New York. https://doi.org/10.1007/s11119-008-9056-2

[22] G.Bohling, "Introduction to geostatistics and variogram analysis," Kansas geological survey, 2005, vol. 1, pp. 1-20.

[23] G.E. Fasshauer, J.G. Zhang, "On choosing "optimal" shape parameters for RBF approximation," Numerical Algorithms, 2007, vol. 45 no. 1-4, pp.345-368.

[24] U.Falchi, C.Parente, G.Prezioso, "Global geoid adjustment on local area for GIS applications using GNSS permanent station coordinates," Geodesy and Cartography, 2018, vol.44, No.3, pp.80-88. https://doi.org/10.3846/gac.2018.4356

[25] E.Alcaras, L.Carnevale, C.Parente, "Interpolating single-beam data for sea bottom GIS modelling," International Journal of Emerging Trends in Engineering Research, 2020, vol.8, No.2, pp.591-597. https://doi.org/10.30534/ijeter/2020/50822020

[26] R.Obrośłak, O.Dorozhynskyy, "Selection of a semivariogram model in the study of spatial distribution of soil moisture", Journal of Water and Land Development, 2017,vol.35, No.1, pp.161-166. https://doi.org/10.1515/jwld-2017-0080

[27] M.P.Batistella Pasini, A.Dal'Col Lúcio, A.Cargnelutti Filho, "Semivariogram models for estimating fig fly population density throughout the year", Pesquisa Agropecuária Brasileira, 2014, vol.49, No.7, pp.493-505.

[28] C.C.G.Correa, P.E.Teodoro, E.D.Cunha, J.D.Oliveira-Júnior, G.Gois, V.M.Bacani, F.E.Torres, "Spatial interpolation of annual rainfall in the State Mato Grosso do Sul (Brazil) using different transitive theoretical mathematical models", International Journal of Innovative Research in Science, Engineering and Technology, 2014, vol.3 No.10, pp.16618-16625.

[29] X.Zhang, L.Jiang, X.Qiu, J.Qiu, J.Wang, Y.Zhu, "An improved method of delineating rectangular management zones using a semivariogram-based technique", Computers and Electronics in Agriculture, 2016, vol.121, pp.74-83.